Source localisation in an unknown reverberant environment using compressive sampling in the frequency domain

Gilles Chardon, Laurent Daudet

Source localisation in an unknown reverberant environment using compressive sampling in the frequency domain

G. Chardon and L. Daudet

Institut Langevin, 10 rue Vauquelin, 75005 Paris, France
gilles.chardon@espci.fr

We introduce a source localisation method dealing with an unknown reverberant environment. The measured acoustic field is decomposed as the sum of a diffuse field and a source field, using a priori knowledge on these fields, i.e. structured sparsity deduced from the governing equations of acoustics. Simulations and experimental results in 2D domains, using greedy algorithms as well as optimisation-based methods, show that the method is robust with respect to noise and sensors localisation. Additionnaly, the density of sensors required can be lower than the Nyquist frequency. These facts make this method an interesting alternative to standard localisation methods particularly when a large number of narrowband sensors are deployed.

1 Introduction

Source localization is a classic problem for which numerous methods have been designed, especially in the free field case where the Green function of the medium is known [1]. In the case of a reverberant environment, existing methods needs a prior knowledge. This knowledge can be a database of pre-measured Green functions [2], or informations about the geometry of the room [3, 4].

Here, we propose a source localisation method dealing with an unknown room, requiring no preliminary calibration. This method is based on a decomposition of the acoustic field as a source component and a reverberated component. Apart from homogeneity and isotropy of the medium (a mild assumption in the case of room acoustics), no further prior knowledge is needed. For instance, boundary conditions or the dispersion relation of the medium can be left unspecified, allowing the application of this method to a wide range of experimental setups (rooms, membranes, plates, etc.).

The price to pay for these performances is a larger number of measurements, placed around the area of interest. Note however that this number is lower than the number of measurements needed for the application of the sampling theorem. Another interesting property of this method, is that it can ignore noise sources located outside of the are of interest, by treating them as a part of the diffuse field.

Note that while here we introduce the method using narrowband measurements, an extension to wideband measurements, requiring more sophisticated modeling, is possible, but left for further research.

Section 2 introduces the model used by the method and section 3 introduces two algorithms based on this model. Simulated and experimental results are given in section 4 and 5, and section 6 concludes the paper.

2 Modeling the soundfield

For the sake of clarity, we will introduce the model in the case of a room Ω with rigid walls. The pressure field $p(\mathbf{x}, t)$ verifies the wave equation:

$$\begin{cases} \Delta p - \frac{1}{c^2}\frac{\partial^2 p}{\partial t^2} = s(\mathbf{x}, t) \\ \frac{\partial p}{\partial n}\Big|_{\partial\Omega} = 0 \end{cases}$$

with c the wave velocity, assumed to be constant in the medium, and $s(\mathbf{x}, t)$ the sources. We assume that the source term is the sum of a few punctual sources at locations $\mathbf{x}_i$:

$$s(\mathbf{x}, t) = \sum_{j=1}^{S} s_j(t)\delta_{\mathbf{x}_j}(\mathbf{x})$$

with $\delta_{\mathbf{x}_j}$ the Dirac mass at point $\mathbf{x}_j$.

After a Fourier transform in time, the wave equation becomes the Helmholtz equation: for all ω, the Fourier transform $\hat{p}(\mathbf{x}, \omega)$ of the pressure verifies

$$\begin{cases} \Delta\hat{p} + k^2\hat{p} = \hat{s} \\ \frac{\partial\hat{p}}{\partial n}\Big|_{\partial\Omega} = 0 \end{cases} \tag{1}$$

where the wavenumber k equals ω/c. The source term is here

$$\hat{s}(\mathbf{x}, \omega) = \sum_{j=1}^{S} \hat{s}_j(\omega)\delta_{\mathbf{x}_j}(\mathbf{x}).$$

In free-field, that is with Sommerfeld boundary conditions, the Green function of the Helmholtz equation is

$$G(\mathbf{x}, \mathbf{x}_j) = \frac{e^{ik\|\mathbf{x}-\mathbf{x}_j\|}}{4\pi\|\mathbf{x}-\mathbf{x}_j\|}$$

and the solution to (1) can be written as a sum of Green functions:

$$\hat{p} = \sum_{j=1}^{S} \hat{s}_j(\omega)G(\mathbf{x}, \mathbf{x}_j).$$

Free-field source localisation method aims at decomposing this solution as a sum of Green function. In a room, direct application of these methods would fail. Indeed, the Green function of a room can be significantly different from the free-field Green function. To deal with this difficulty, we suggest to reduce source localisation in a room to a problem close to free-field source localisation, by carefully modeling and manipulating the data.

To this end, we decompose the solution of equation 1 as a free-field solution $\hat{p}_s$, sum of the free-field Green function at points $\mathbf{x}_j$ plus a correction term $\hat{p}_0$, solution of the homogeneous Helmholtz equation, such that the sum verifies the boundary conditions:

$$\hat{p}_s(\mathbf{x}, \omega) = \sum_{j=1}^{S} \hat{s}_j(\omega)G(\mathbf{x}, \mathbf{x}_j)$$

$$\begin{cases} \Delta\hat{p}_0 + k^2\hat{p}_0 = 0 \\ \frac{\partial\hat{p}_0}{\partial n}\Big|_{\partial\Omega} = -\frac{\partial\hat{p}_s}{\partial n}\Big|_{\partial\Omega} \end{cases}$$

These two components have distinct models: the first is a sum of a few Green functions, while the second is an homogeneous solution of the Helmholtz equation. This will allow us to separate their contributions in experimental measurements.

Before going further, we will slightly modify the decomposition, trading physical meaning for better mathematical properties: the Green function G is proportionnal to the Hankel function of order 0:

$$G(\mathbf{x}, \mathbf{x}_j) = \frac{ik}{4\pi}h_0(k\|\mathbf{x}-\mathbf{x}_j\|)$$

This Hankel function h_0 is actually a combination of the Bessel functions of first kind j_0 and second kind y_0:

$$h_0(kr) = j_0(kr) + iy_0(kr)$$

The former is a solution of the homogeneous Helmholtz equation and will be included in p_0. The latter is then used as the source term. This decomposition writes:

$$\hat{p}_s(\mathbf{x}, \omega) = \frac{ik}{4\pi} \sum_{j=1}^{S} \hat{s}_j(\omega) y_0(k\|\mathbf{x} - \mathbf{x}_j\|)$$

$$\begin{cases} \Delta \hat{p}_0 + k^2 \hat{p}_0 = 0 \\ \frac{\partial \hat{p}_0}{\partial n}\Big|_{\partial\Omega} = - \frac{\partial \hat{p}_s}{\partial n}\Big|_{\partial\Omega} \end{cases}$$

The homogeneous term $\hat{p}_0$ can be approximated by a sum of plane waves or Fourier-Bessel functions [5]. The number L of plane waves needed to approximate $\hat{p}_0$ is significantly lower than the size of the discretization needed by the sampling theorem or standard numerical methods like finite differences or finite elements: it scales like k while standard discretisation sizes scale like k^2.

The final decomposition of the acoustic field writes

$$\begin{array}{ccccc} \hat{p} & = & \hat{p}_0 & + & \hat{p}_s \\ \hat{p} & \approx & \sum_{l=1}^{L} \alpha_l e_l(\mathbf{x}) & + & \sum_{j=1}^{S} \hat{s}_j(\omega) y_0(k\|\mathbf{x} - \mathbf{x}_j\|). \end{array}$$

where the e_l are plane waves $\exp(i\mathbf{k}_l \cdot \mathbf{x})$ with wave vectors $\mathbf{k}_l$ drawn on the sphere of radius k. The unknowns are α_l, the coefficients of the decomposition of the diffuse field, $\hat{s}_j(\omega)$ and $\mathbf{x}_j$, the amplitude and positions of the sources, to be determined. Note that the information we are interested in (positions of the sources) is contained in $\hat{p}_s$. After removal of this diffuse field, the problem is very similar to free-field localisation.

While this mathematical analysis has been carried out for a room with rigid walls, it does not depend on the boundary conditions. For instance, the decomposition can be done in a subset of the room. In this case, only sources inside the convex hull of the measurements will be included in the source term, sources outside the antenna will be included in the diffuse component and not be considered.

3 Algorithms

The source field $\hat{p}_s$, being the sum of few contributions of punctual sources, is a sparse vector: it can be approximated by a sum of few atoms drawn from a pre-determined dictionnary. Sparse recovery algorithms have been developped to recover the original sparse vector from measurements, and have already been applied to source localisation [1, 6]. In the general case, they aim at recovering a sparse vector $\mathbf{s}$ from measurements $\mathbf{m} = \mathbf{Dx}$ where $\mathbf{D}$ is a matrix, called dictionary, modeling informations about the measurement process and the signal model.

Most of them fall in two categories:

- optimisation-based methods, aiming at recovering the solution as the minimizer of a carefully chosen criterion,

- iterative algorithms, identifying the components of the signal one by one.

Here, we use variations of the algorithms to deal with the slightly more complex sparse model describing the acoustic fields.

The vector we have to decompose is the vector of measurements of $\hat{p}$ at points $\mathbf{x}_m$ that we will call $\mathbf{p}$. The dictionnary is made of two sub-dictionnaries:

- A plane wave dictionnary $\mathbf{W}$, with L plane waves sampled at points $\mathbf{x}_m$. Its (m, l)-term is $w_{ml} = \exp(i\mathbf{k_l} \cdot \mathbf{x}_m)$.

- A source dictionnary $\mathbf{S}$, with sources located at candidate locations $\mathbf{y}_m$, sampled at points $\mathbf{x}_m$. Its (m, j)-term is $s_{mj} = y_0(k\|\mathbf{y}_j - \mathbf{x}_m\|)$.

The vector of measurements $\mathbf{p}$ then writes

$$\mathbf{p} = \mathbf{W}\alpha + \mathbf{S}\beta$$

where β is assumed to be sparse: the nonzero terms in β indicate the source. The number of nonzero terms, i.e. the number of sources, is assumed to be small. No priors are imposed on α.

3.1 Greedy source localisation algorithm

The first algorithm we propose is an iterative algorithm based on Orthogonal Matching Pursuit. This algorithm identifies the nonzero components of the vector one by one, by choosing, at each step, the atom the most correlated with the signal, and removing its contribution. Here, this method would fail, as the correlation of the field with the source dictionnary is perturbed by the diffuse field.

The source localisation algorithm follows the same global strategy, after removal of the homogeneous term, by projecting the signal on the orthogonal of the space spanned by plane waves.

Note that, in the outline of the algorithm, $\mathbf{W}^\dagger$ denotes the Moore-Penrose pseudo-inverse of $\mathbf{W}^\dagger$, and that $\left(\mathbf{W}|\mathbf{s}_{\mathbf{y}_j}\right)$ is the concatenation of the matrix $\mathbf{W}$ and the vector $\mathbf{s}_{\mathbf{y}_j}$.

Algorithm 1 Greedy source localization algorithm

Input: measurements $\mathbf{p}$, number of sources n, plane waves dictionary $\mathbf{W}$, source atoms $\mathbf{s_y}$
Output: estimated positions of the sources $\mathbf{y}_j$
  $\mathbf{p}_s \leftarrow \mathbf{p} - \mathbf{WW}^\dagger\mathbf{p}$
  for $j = 1$ to n **do**
    $\mathbf{y}_j \leftarrow \max_{\mathbf{y}} \left|\left\langle \mathbf{s_y}, \mathbf{p}_s \right\rangle\right|$
    $\mathbf{W} \leftarrow \left(\mathbf{W}|\mathbf{s}_{\mathbf{y}_j}\right)$
    $\mathbf{p}_s \leftarrow \mathbf{p} - \mathbf{WW}^\dagger\mathbf{p}$
  end for

3.2 Group Basis Pursuit

The most representative algorithm of this category is Basis Pursuit [7]. It recovers the sparse vector $\mathbf{s}$ as the solution of the optimisation problem:

$$\mathbf{s} = \text{argmin}\|\mathbf{s}\|_1 \text{ such that } \mathbf{m} = \mathbf{Ds}.$$

The ℓ_1 norms acts as a proxy to the ℓ_0 norm, counting the number of nonzero coefficients in $\mathbf{x}$, but unfortunately nonconvex. Minimisation of different criterions can be used in the case of more complicated sparsity models.
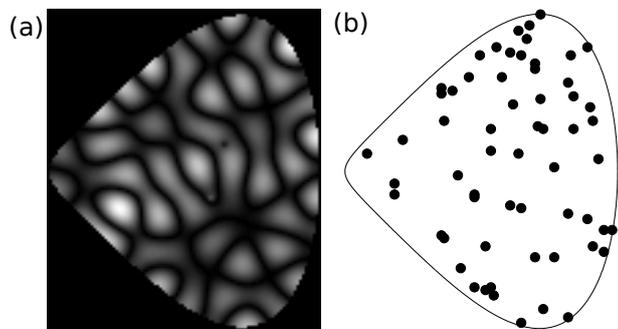
Figure 1: Numerical simulations : (a) Modulus of the simulated field (b) Position of samples used for the localization

Here, we solve the minisation problem

$$(\hat{\alpha}, \hat{\beta}) = \min_{\alpha, \beta} \|\alpha\|_2 + \|\beta\|_1 \quad \text{s.t.} \quad \|\mathbf{W}\alpha + \mathbf{S}\beta - \mathbf{p}\| < \epsilon$$

with ϵ being the amount of noise expected in the measurements. The ℓ_2 norm on α means that it has not to be sparse while the ℓ_1 norm on β promotes its sparsity.

4 Numerical simulations

To test the algorithms, we first use simulated data. For better visualisation, these are run in 2D. The theoretical analysis still holds, replacing spherical Bessel function j_0, y_0 and h_0 by their cylindrical counterparts J_0, Y_0 and H_0. We use FreeFem++ [8], a finite element solver, to simulated the wave propagation in a membrane with Dirichlet boundary conditions. Two sources are in the membrane, and 60 measurements are used. The simulated field and the locations of the measurements are plotted figure 1

4.1 Greedy algorithm

An estimation of the decomposition of the field as a source component plus a diffuse component is shown figure 2. It is obtained by projecting the field on the space spanned by the plane waves. Application of a free-field source localisation method here fails, as can be seen figure 3 (a): the correlations of the atoms and the measurements do not allow the localization of the sources, because of the mismatch between the model and the physical setup. More precisely, the correlation with the complete field is the sum of the correlation with the diffuse field and the source field. As the diffuse field can be significantly larger than the source field, e.g. near a eigenfrequency, its correlation with the measurements, meaningless, corrupts the estimation.

Results of the proposed algorithm are shown figure 3 (b,c,d): correlations after removal of the diffuse field at the first step and second step allow a correct estimation of the source locations. The true localisations and their estimations are plotted figure 3 (d).

While this not its main purpose, the algorithm can reconstruct the field in the entire membrane, by using the estimated decomposition of the field to compute the value at any point in the membrane. This reconstruction is shown figure 4
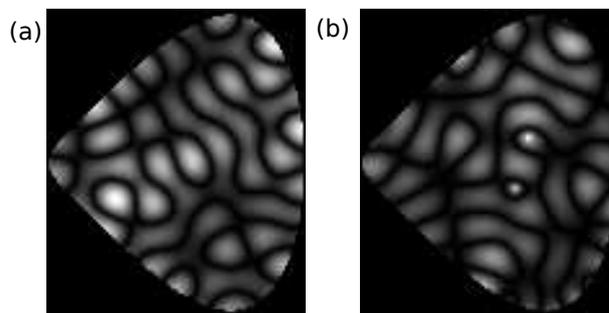

Figure 2: Numerical simulations : Decomposition of the measurements as (a) diffuse component p_0 and (b) source component p_s

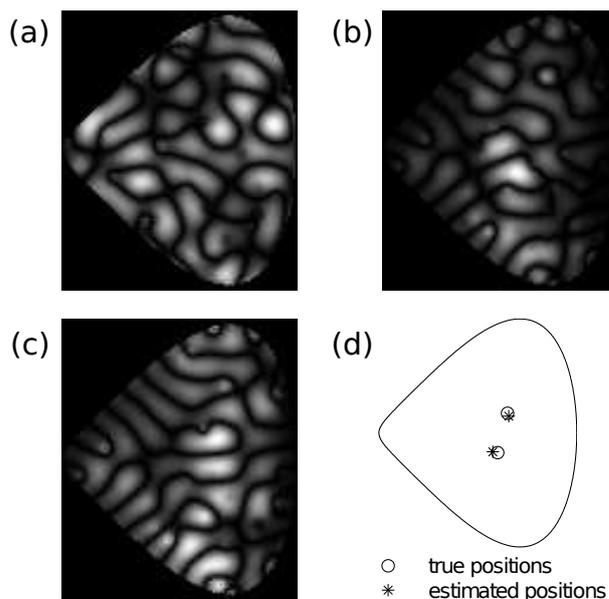○ true positions
∗ estimated positions

Figure 3: Numerical simulations : Correlations at the first step of the greedy algorithm (a) before and (b) after the projection. (c) Correlations at the second step. (d) Estimated source positions.
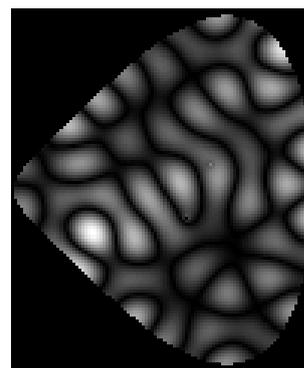

Figure 4: Reconstruction of the field from the measurements

4.2 Group Basis Pursuit

As expected, direct application of Basis Pursuit with a free-field model fails (cf. figure 5 (a)). Here the two sources are visible, but a lot of artifacts appear near the borders. These can be explained by a tentative of Basis Pursuit to explain the acoustic field as a sum of fundamental solutions, similarly to what is done in the Method of Fundamental Solutions [9]. In this method, the sources would be located out-

side of the domain of interest. Here, this is approximated by sources near the boundaries. Correct modeling of the acoustic field, with a modified criterion, yields accurate localization of the sources without artifacts (figure 5 (b). Both Basis Pursuit and Group Basis Pursuit are solved using the `spgl1` toolbox [10] [11].
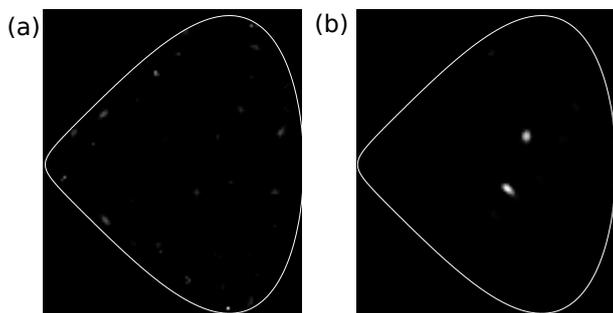

Figure 5: Numerical simulations : Sources estimated by (a) basis pursuit with sources dictionary (b) group basis pursuit with plane waves and sources dictionary

5 Experimental results

Experimental results are obtained using a metallic plate, with one source (Figure 6 (a)). The plate is excited by a piezoelectric transducer, and a laser vibrometer measures its normal displacement. The behaviour of this displacement is given by the Kirchhoff-Love equation

$$D\Delta^2 w + 2\rho h \frac{\partial^2 w}{\partial t^2} = f$$

where D is the bending stiffness of the plate, ρ its density, h its thickness and f the normal force applied to the plate. Although it does not really match with the model described at the beginning of the paper, it can be shown, that the plane wave decomposition still holds away from the boundaries [12]. Indeed, the normal displacement can be approximated by sum of plane waves and evanescent waves, which can be neglected away from the borders without any significant loss of precision. Source terms are sums of Bessel functions and modified Bessel functions, but these will be neglected here.

Another difficulty is the fact that the dispersion relation of the plate is not know, and needs to be estimated. We use the method describe in [12]. While it was designed for homogeneous solutions, the presence of the source field, weak compared to the diffuse field in this case, does not perturb the estimation.

The normal displacement is sampled on a regular grid of 64 samples, with sampling period of 32mm, higher that what would be prescribed by the sampling theorem: at frequency $f = 30631$ Hz, the estimated wavelength is 49.4mm, and the largest possible sampling period would be 24.7mm. As shown in [12], this has no significant effect on the estimation of the wavenumber or of the diffuse field. The samples used and the amplitudes of the signals are shown figure 7.

Greedy algorithm: As there is only one source, we use only one step of the algorithm. The correlations at the first step of OMP (figure 8 (a)) does not allow the localisation of the source. After projection, the maximum of the correlations
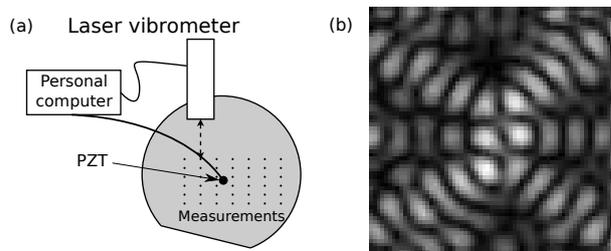

Figure 6: (a) Experimental setup (b) Amplitude of the field measured at frequency $f = 30\,631$ Hz on a 4mm sampling grid.
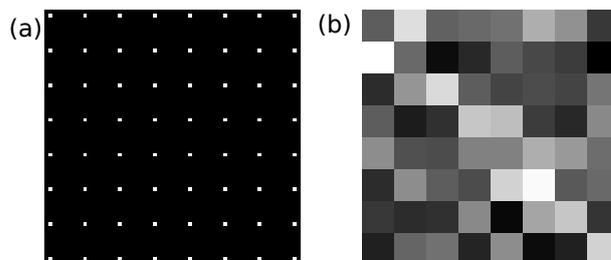

Figure 7: (a) Uniform sub-Nyquist sampling used for localization (b) Amplitude of the corresponding measured subsampled field
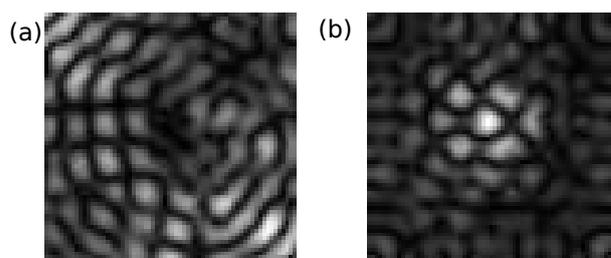

Figure 8: Correlations at the first step of the greedy algorithm (a) before and (b) after the projection, on the experimental data.
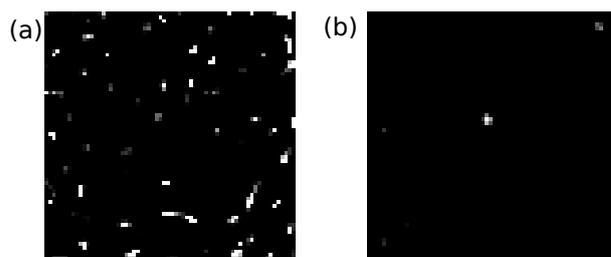

Figure 9: Source position and amplitude estimated by (a) basis pursuit (source-only dictionary) (b) group basis pursuit (full dictionary)

is clearly at the center, where the plate was excited (figure 8 (b)).

Group Basis Pursuit: Localisation with the free-field dictionnary fails, with results worse than what was obtained in the simulations (figure 9 (a)): the true source is not even visible. However, with Group Basis Pursuit and the complete dictionnary, the source is correctly recovered at the center (figure 9 (b)).

6 Conclusion

A new source localisation method was introduced, dealing with an unknown reverberant environment and narrowband measurements. Extension to wideband signals, or more precisely multiple narrowband signals, with joint sparsity across frequencies, will be investigated, as well as localisation of directional sources, using a dictionnary of spherical harmonics and a modified sparse mode. Some issues still need to be resolved, such as the number of microphones needed as well as their optimal placement. Finally comparison with other source localisation with reverberation will be done

7 Acknowledgements

References

[1] D. Malioutov, M. Cetin, and A. S. Willsky, "A sparse signal reconstruction perspective for source localization with sensor arrays," *IEEE Trans. Sig. Proc.*, vol. 53, no. 8, 2005.

[2] R.-K. Ing, N. Quieffin, S. Catheline, and M. Fink, "In solid localization of finger impacts using acoustic time-reversal process," *Applied Physics Letters*, vol. 87, no. 20, 2005.

[3] S. Nam and R. Gribonval, "Physics-driven structured cosparse modeling for source localization," in *Proceedings of the International Conference on Acoustics, Speech and Signal Processing, Kyoto, Japan*, 2012.

[4] I. Dokmanic and M; Vetterli, "Room helps: acoustics localisation with finite elements," in *Proceedings of the International Conference on Acoustics, Speech and Signal Processing, Kyoto, Japan*, 2012.

[5] A. Moiola, R. Hiptmair, and I. Perugia, "Plane wave approximation of homogeneous Helmholtz solutions," *Zeitschrift für Angewandte Mathematik und Physik*, vol. 62, 2011.

[6] A. Peillot, F. Ollivier, G. Chardon, and L. Daudet, "Localization and identification of sound sources using "compressive sampling" techniques," in *Proceedings of the 18th International Congress on Sound and Vibration, Rio de Janeiro, Brazil*, 2011.

[7] S.S. Chen, D.L. Donoho, and M.A. Saunders, "Atomic decomposition by basis pursuit," *SIAM J. Sci. Comp.*, vol. 20, 1998.

[8] O. Pironneau, F. Hecht, Le Hyaric A., and Morice J., "FreeFem++," http://www.freefem.org/ff++.

[9] G. Fairweather and A. Karageorghis, "The method of fundamental solutions for elliptic boundary value problems," *Adv. Comp. Math.*, vol. 9, 1998.

[10] E. van den Berg and M. P. Friedlander, "SPGL1: A solver for large-scale sparse reconstruction," June 2007, http://www.cs.ubc.ca/labs/scl/spgl1.

[11] E. van den Berg and M. P. Friedlander, "Probing the Pareto frontier for basis pursuit solutions," *SIAM Journ. Sc. Comp.*, vol. 31, no. 2, 2008.

[12] G. Chardon, A. Leblanc, and L. Daudet, "Plate impulse response spatial interpolation with sub-Nyquist sampling," *Journ. Sound Vibration*, vol. 330, no. 23, 2011.